Macromolecular Research, Vol. 23, No. 9, pp 795-801 (2015)
DOI 10.1007/s13233-015-3110-5

www.springer.com/13233
pISSN 1598-5032 eISSN 2092-7673

Enhanced Thermoelectric Performance of CNT Thin Film p/n Junctions Doped with N-Containing Organic Molecules

Hyunwoo Bark[1], Wonmok Lee[2], and Hyunjung Lee*[,1]

[1]*School of Advanced Materials Engineering, Kookmin University, Jeongneungro 77, Seoul 136-702, Korea*
[2]*Department of Chemistry, Sejong University, 98 Gunja-Dong, Gwangjin-Gu, Seoul 143-747, Korea*

Received January 27, 2015; Revised June 10, 2015; Accepted June 20, 2015

Abstract: Despite the high thermoelectric performance of traditional inorganic semiconductors-based thermoelectric materials, recent efforts have been made to utilize the unique advantages of organic thermoelectric materials. Carbon-based organic thermoelectric materials are considered as an economically viable option, offering the advantages of large area fabrication, flexible and lightweight modules, in addition to their low thermal conductivity required for superior thermoelectric performance. The limitation of low electrical conductivity of organic materials could be circumvented by forming a percolating network of single walled carbon nanotubes (SWNTs) in the form of buckypaper. In this study, buckypapers were prepared by vacuum filtration of acid-treated SWNTs, which provided a percolating network for efficient electron transport. Subsequently, p-type and n-type buckypapers were prepared by acid treatment or reduction by urea moelecules or encapsulating SWNTs with electron donating organic compounds like polyethylenimine. The thermoelectric properties of the buckypapers were analyzed as a function of temperature. The acid-treated SWNTs and urea-SWNTs generated positive thermopower of up to 60 μV/K at 380 K, and hence were used as p-type thermoelectric materials. On the other hand, the polyethylenimine-SWNT generated negative thermopower of -60 μV/K at 380 K, used as n-doped material. Subsequently, thermoelectric module was fabricated by alternatively stacking the p-type and n-type buckypapers. Each p-n couple generated a thermoelectric voltage of 0.7 mV per temperature gradient of 50 K. With an increase in the number of p-n layers to four, the thermoelectric voltage increased to 7 mV for a temperature gradient of 50 K. This module generated a power upto 960 nW upon varying load resistance due to their low electrical resistance formed by well percolated networks of SWNTs. The higher electrical conductivities of p-type and n-type SWNTs were achieved by incorporating organic materials such as reducing agent (urea) or electron donating functional groups (PEI) around the surface of SWNTs, respectively.

Keywords: carbon nanotubes, flexible composites, thermoelecric modules.

Introduction

A thermoelectric power generator is an effective renewable energy source that directly converts waste heat into useful electric power. The thermoelectric modules, which constitute the thermoelectric generator, convert the temperature gradient into electrical energy, based on the "Seebeck effect." In principle, a temperature gradient in the thermoelectric module (ΔT) induces the diffusion of charged carriers (electrons or holes) from the hot side to cold side. As a result, the potential (ΔV) is generated.[1] The efficiency of a thermoelectric generator is indicated by the figure of merit (ZT), defined as $(S^2 \cdot \sigma)/\kappa$. Here, S, σ, κ, and T represent the Seebeck coefficient, electrical conductivity, thermal conductivity, and absolute temperature, respectively. According to this equation, high-performance thermoelectric generators demand superior thermoelectric materials with high electrical conductivity, high Seebeck coefficient, and low thermal conductivity.

For several decades now, bulk bismuth chalcogenides, lead telluride, and tellurium based thermoelectric materials have been actively studied as high-performance thermoelectric materials.[2-6] However, these semiconductor thermoelectric materials have certain inherent limitations. For instance, the above mentioned semiconductors are associated with challenges in large-area fabrication and stacked structure owing to their brittleness. In addition, they are highly expensive. To overcome these limitations, some researchers have proposed the use of alternative materials, such as electrically conducting organic materials, carbon nanotubes (CNT), graphenes and polymer composites.[7-16] Compared to conventional semiconductor-based thermoelectric materials, these organic materials are flexible, lightweight, and require simple low-temperature processes

*Corresponding Author. E-mail: hyunjung@kookmin.ac.kr

for large-area fabrication. In particular, several reports have suggested the possibility of realizing higher figure of merit with CNTs owing to their outstanding mechanical properties and electrical conductivity.[17-21] To this end, recent studies have focused on the fabrication of CNTs/polymer composite, wherein CNTs provide high electrical conductivity and polymer provides thermal insulation, thereby decreasing thermal conductivity. Above the percolation threshold of CNTs in polymer matrix, it has been reported that high electrical conductivity could be achieved only with small amount of CNTs.[22] Lately, Yu and Grunlan *et al*. have demonstrated an enhancement in the thermoelectric properties of CNT-filled polymer composites by modifying the junctions between CNTs using poly(3,4-ethylenedioxythiophene) poly(styrenesulfonate) (PEDOT:PSS).[19,20] The thermoelectric module was made of p-typed and n-typed thermoelectric materials of carbon nanotubes and polymer composites. Here, the PEDOT:PSS particles tend to localize at the junction of CNTs, thereby promoting the electron transportation and preventing the heat transfer due to their high electrical conductivity and low thermal conductivity. As a result, the composite showed a high electrical conductivity of up to ~40000 S/m, while their Seebeck constant and thermal conductivity remained relatively constant. Recently, Carroll *et al*. reported a multilayered carbon nanotube/polymer composite, in which each p/n couple was composed of two films made of polyvinylidene fluoride with 95 or 20 wt% of multi-walled carbon nanotubes.[23] A single conducting layer produced ~15 μV per 1 K temperature gradient. Thermoelectric modules made of carbon nanotube/cellulose fiber composites were fabricated with one, two, and three p-n couples connected in series.[20] The testing modules produced ~6 mV thermoelectric voltage, with ~25 nW of power generated for a temperature gradient of ~22 K.

In principle, thermoelectric module consists of alternating structures of p-typed and n-typed thermoelectric materials. As-grown pristine CNTs inherently tend to exhibit p-type conductivity owing to the presence of -OH or CO_2H on their surface defects.[24,25] Oxidization of CNTs in acidic solution will further enhance their p-type characteristics due to the formation of carboxylic acid groups on their surface. On the other hand, n-type CNTs is typically achieved by doping with alkaline-earth metals, nitrogen, potassium, or iodine.[26,27] Nevertheless, these n-doped CNTs are unstable in the air and suffer from low degree of doping. Alternatively, n-type CNTs could be prepared by functionalizing CNTs with organic materials, which are stable in air and contain excess electrons. Among them, polyethylenimine (PEI) has been considered to be an effective p-type dopant in the field of transistors.[28] PEI contains several amine groups that are characterized by a lone pair of electrons, making them ideal p-type donors for CNTs. Urea has been used as an environmentally friendly and a mild reducing agent to reduce graphene oxide to stale reduced grapheme oxide.[29] Therefore, CNTs, graphene analogues also can be reduced partially with urea-treatment.

In this paper, we report the thermoelectric properties of single-walled carbon nanotubes (SWNTs)-based composite, fabricated in the form of a thin film thermoelectric module. Pristine SWNTs were treated in acidic solution and fabricated in the form of buckypapers. Subsequently, p-type and n-type doping was realized by dip coating in urea solution and PEI solution, respectively. The thermoelectric properties of acid-treated SWNTs (p-type, P1), SWNTs dip-coated in urea solution (p-type, P2), and SWNTs dip-coated in PEI solution (n-type, N) were analyzed. In addition, a thermoelectric module was fabricated by alternate stacking of the p-type and n-type buckypapers (Figure S1). Our results show that the limitation of low electrical conductivity of organic materials could be circumvented by a pre-formed percolating network of SWNTs in the form of buckypaper.

Experimental

Materials. Commercially available single-walled carbon nanotubes (SWNTs, ASP-100F) of diameter 1-2 nm were purchased from Hanhwa Nanotech Inc., Republic of Korea. Commercial SWNTs were produced by arc discharge method and subsequently purified by thermal and acid treatment. Carbonaceous impurities formed during the arc discharge process, such as amorphous carbon and carbon nanoparticles, were removed during the thermal treatment. In addition, the acid treatment was used to remove the metallic catalyst employed during the synthesis process. The SWNTs were used as purchased, without any other treatment. However, the as-obtained SWNTs were referred to as "acid-treated SWNT" in this study, in order to emphasize the existence of carboxylic acid on the surface of SWNT. Urea (NH_2-CO-NH_2) and PEI (M_w: ~25,000) were purchased from Sigma-Aldrich. All chemicals were used as received.

Fabrication of CNT Buckypapers. 20 mg of acid-treated SWNTs were dispersed in 50 mL of ethanol for 30 min, using an ultrasonic agitator (750 W, Sonics & Materials Inc.) with cooling bath. Subsequently, CNTs were filtered using a PTFE membrane filter (0.2 μm, ϕ=47 mm) and dried in a vacuum oven at 313 K for 24 h in order to remove ethanol. The buckypapers thus obtained were p-doped and n-doped by immersing in aqueous solution of urea (10 wt%) and PEI solution in ethanol (10 wt%), respectively, for 24 h. Finally, the p-doped buckypapers were dried in a vacuum oven at 353 K for effective removal of water, while the n-doped buckypapers were dried at room temperature.

Fabrication of Thermoelectric Module. The thickness of as-obtained bucky paper with acid-treated SWNTs was approximately 20 μm. After dip coating in PEI and urea solution, the thickness of the n-doped bucky paper increased to 70 and 80 μm, respectively. All the bucky papers (acid-treated, p-doped, and n-doped) were cut into sheets of dimension 20× 20 mm. The thermoelectric module was fabricated by stacking the bucky papers between an insulating layer (double-side

sticky tape, 3M). Every other bucky paper contains p-type CNTs, while the others contain n-type CNTs, so as to form a p-n junction. The shorter insulating layers allowed for alternating p/n junctions when the silver paste (TEC-PA-040, InkTec Co., Etd, Korea) was placed between p-n junctions, which were minimizing the interfacial resistance. The thermoelectric module was fabricated by repeating this stacking sequence up to four times.

Characterization. The amount of urea and PEI molecules attached to the surface of acid treated SWNT was estimated by using thermo gravimetric analysis (TGA, STA-1500, TA Instruments, U.S.A), conducted in air atmosphere at a heating rate of 10 K/min. In addition, compositional analysis of the thin film (10×10 mm) was performed by X-ray photoelectron spectroscopy (XPS, ESCA 2000, VG Microtech, England), using twin anode Mg/Al as the X-ray source. The electrical conductivity and Seebeck coefficient were determined at 298, 323, 348, and 373 K by using four-point-probe method. (Figure S2) Four points were placed at a same interval on the surface of a sample film. A direct current (DC) precision current source (Keithley 2400, Keithley Instruments, Inc., United States) and nanovoltmeter (Agilent 34420A, Agilent Technologies, Inc., United States) were used for all measurements. The sheet resistance obtained from the current-voltage measurement was converted into electrical conductivity with a dimensional factor. The Seebeck coefficient was measured from the slope of the temperature-voltage graph. The temperature gradient was applied across the surface of a sample film by ceramic heating block, and the type-R thermocouple (+: Pt/Rh=87/13, w/w, -: Pt) was used in measuring temperature. The temperature was detected by data acquisition/data logger switch unit (Agilent 34970A, Agilent Technologies, Inc., United States). The potential was plotted against the temperature difference (ΔT) at a specified temperature ± 3 K, the slope of which yielded the Seebeck coefficient. In order to determine the reliability of electrical conductivity and Seebeck coefficient, we surveyed the electrical conductivity and Seebeck coefficient of Ni (99.99%). The electrical resistivity and Seebeck coefficient of Ni were measured as 6.9×10^{-6} Ω·m and -21.5 μV/K at room temperature, respectively. These data are a good agreement with a literature report.[30] The linear least squares in calculating Seebeck coefficient were larger than 0.99. The power factor was calculated by multiplying the square of Seebeck coefficient and electrical conductivity.

In order to investigate thermoelectric properties of modules consisting of n-type and p-type SWNT bucky papers, electrical resistance, Seebeck coefficient, generated thermoelectric voltage and power output depending on temperature gradient were surveyed. For electrical resistance, platinum (Pt, diameter=76 μm) wires were attached at each side of a module and they were connected with a nanovoltmeter and a current source for a four-wire resistance method. The Seebeck coefficient of the modules was obtained by similar method with that of each bucky paper. The electrical resistance and Seebeck coefficient were detected from 298 to 373 K. Generated thermoelectric voltage was obtained by applying ΔT=5, 10, 15, 20, 25, 30, 35, 40, 45, and 50 K. For power output, generated thermoelectric voltage (V_{TEP}) was monitored for varying load resistance (R) at ΔT=50 K, and power output (P) was calculated by $P=V_{TEP}^2/R$.

Results and Discussion

One of the most important outcomes from the present study is a successful fabrication of thermoelectric modules with all carbon-based materials, such as SWNT, polymer, functional organic compounds and so on.

Thermal gravimetric analysis (TGA) was performed to determine the amount of urea and PEI attached to the surface of SWNTs. As evidenced from Figure 1(a), pure urea molecules decompose at ~450 and 520 K, analogous to the values reported in the literature.[31] At 450 K, the urea molecules decompose into ammonia (NH_3) and fulminic acid (HCNO). Considering the decomposition of urea at 450 K, the weight percentage of urea-SWNTs (P2) was calculated to be ~18 wt%.

In addition, we also estimated the weight percentage of PEI attached on SWNTs (N). As can be seen from the TGA curve, acid-treated SWNTs (P1) decomposed at ~750 K, which indicates a PEI weight percentage of 20 wt%. Furthermore, from the TGA data, we confirmed that there was no loss of urea or PEI in the temperature range of 300-370 K, so as to ensure that the thermoelectric properties are determined without the thermal decomposition of urea or PEI.

Furthermore, XPS was employed to determine the chemical composition and the nature of chemical bonds present on the surface of acid-treated SWNTs and urea-SWNTs, respectively. The dip-coated PEI was already revealed to be physically adsorbed on the surface of SWNTs.[28] The C 1s XPS spectrum of acid-treated SWNTs (P1) shown in Figure 1(b) indicates the predominant presence of C-C (sp^2 and sp^3). Besides, several functional groups containing oxygen atoms, such as C-OH and COOH, were also detected, which are believed to be developed upon treatments with acid. After urea-treatment, the XPS spectrum of urea-SWNT (P2) in Figure 1(c) contains additional peaks for C=O bonding, and N-containing functional groups (C-N and N-C=O) as well as the same peaks shown in Figure 1(b). These are expected to come from the adsorbed urea molecules on the surface of SWNTs. In order to estimate the reducing effect of urea, the peak of C-C (sp^2 and sp^3) was divided by the area of oxygen containing groups of C-OH and COOH respectively and compared the values in P1 and P2 to indicate the change of SWNT surface structures after urea treatment. At this point we excluded the area of C=O because they came from the adsorbed urea molecules. The ratio was incresed from 4.0 to 5.7, which means C-OH and COOH were partially reduced to C-C and defects in SWNTs were healed effectively. The main peak of urea-SWNTs in

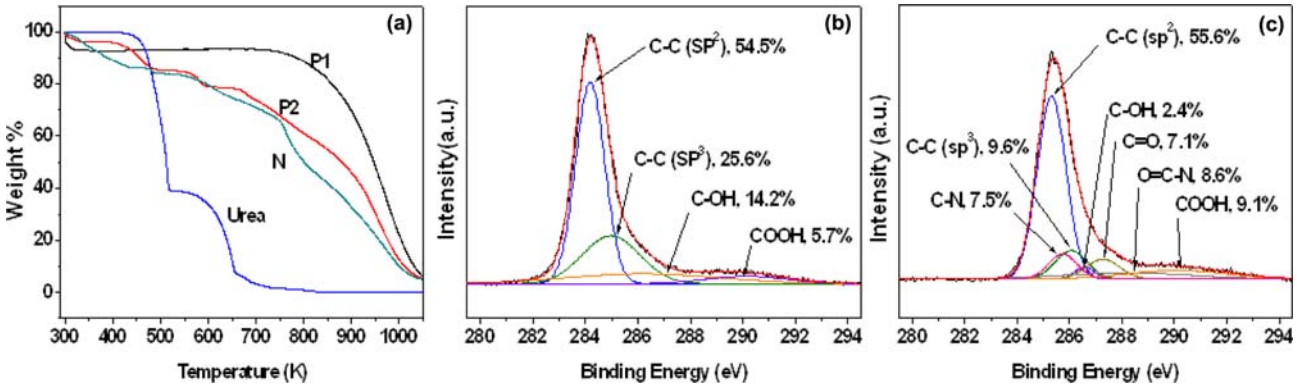

Figure 1. (a) TGA analysis of urea, acid-treated SWNT (P1), urea-SWNT (P2), and PEI-SWNT (N). XPS analysis of (b) acid-treated SWNT (P1), and (c) urea-SWNT (P2).

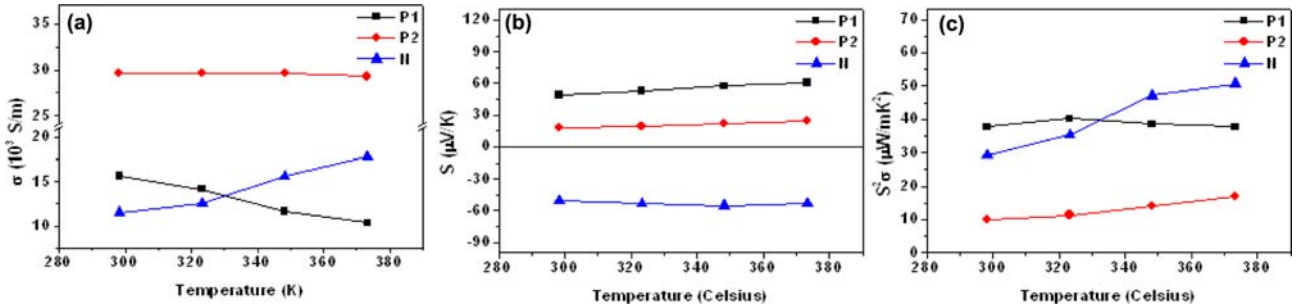

Figure 2. (a) Electrical conductivity (σ), (b) Seebeck coefficient (S), and (c) power factor ($S^2\sigma$) of acid-treated SWNT (P1), urea-SWNT (P2), and PEI-SWNT (N).

Figure 1(c) was found at 285.3 eV of binding energy, which was about 1.1 eV larger than that of acid treated SWNTs (284.2 eV). This shift is ascribed to an increase of electronic density in SWNTs, because of partial reduction of SWNTs by urea or an electron donating effect by amine functional groups in urea molecules.[32]

The thermoelectric properties of acid-treated SWNTs (P1), urea-SWNTs (P2), and PEI-SWNTs (N) were investigated at 293, 323, 348, and 373 K. As evidenced from Figure 2, urea-SWNTs (P2) showed electrical conductivity upto ~ 30000 S/m which is larger than those of acid-treated SWNTs (P1) and PEI-SWNT (N) owing to effective electron transport through the healed defects on SWNT walls by urea molecules. It shows no remarkable change up to 373 K. For the case of PEI-SWNTs (N), the slight decrease in electrical conductivity could be explained by light n-type doping mechanism, which was also confirmed by a lowered Seebeck coefficient upon PEI treatment.[33]

Although urea-SWNTs (P2) didn't show any temperature dependence on electrical conductity from 293 to 373 K, the electrical conductivity of acid-treated SWNT (P1) was decreased from 15000 to 10000 S/m, whereas that of PEI-SWNT (N) was increased from 11000 to 18000 S/m. In general, the electrical conductivity of SWNT bucky papers can be explained by intermolecular trasport between nanotubes as well as charge carrier diffusion. The electrical conductivity of the interconnected network of SWNT could be explained on the basis of two independent mechanisms, namely, fluctuation-induced tunneling mechanism and hopping transport mechanism.[34] The dominant mechanism could vary, depending on the temperature ranges. At low temperatures, the electron transport is dominated by hopping mechanism. On the other hand, the electrical conductivity of SWNTs network is governed by fluctuation-induced tunneling conduction at high temperatures, due to the thermally activated fluctuations of electrons. However, transport of phonons (*i.e*. conductor of heat) is increased at higher temperature, as well as that of thermally activated electrons. As a result, backscattering of charged carriers caused by phonons is also enhanced at higher temperature, which causes a decrease in electrical conductivity. In the case of acid-treated SWNTs, backscattering of carriers by phonons was enhanced because of high thermal expansion coefficient.[35] Additionally, the van der Waals force among bundled SWNTs became weaker at high temperatures, hindering the tunneling of electrons. Eventually, the electrical conductivity of acid-treated SWNTs decreased at an elevated temperature. On the other hand, the electrical conductivity of PEI-SWNT was found to increase at higher temperature. Here, PEI not only acts as an n-type dopant increasing the concentration of electrons into CNTs, but also acts as an insu-

lating layer. In other words, the electrical conductivity of PEI-SWNT increased due to the fluctuation-induced tunneling at high temperatures,[36] as the backscattering of charged carriers caused by phonons was reduced due to its insulating effect. Among the three samples analyzed in this study, urea-SWNT showed the highest electrical conductivity, without any significant change in the whole range of temperature. It is believed that the reduction of acid-treated SWNTs by urea molecules provided much more effective sp^2 structures, thereby increasing the electrical conductivity upto 30000 S/m.

Unlike the temperature dependence of electrical conductivities, the absolute values of Seebeck coefficients showed a slight increase from 298 to 373 K for both n-type and p-type samples. In case of acid-treated SWNTs(P1), the Seebeck coefficient increased from about 50 to 60 μV/K between 298 and 373 K. On the other hand, the Seebeck coefficients of urea-SWNT (P2) were lower than those of acid-treated SWNT(P1) in the entire temperature range. These results were supported by the observed carrier concentration of urea-SWNTs (~ 6×10^{22} cm^{-3}) which was twice as high as that of aicd-treated SWNTs (Figure S3). As we urged above, an increase of electron concentration results in the low Seebeck voltages. Furthermore, the Seebeck coefficient of PEI-SWNT (N) was found to be -50 μV/K at 298 K, and their absolute values increased slightly at higher temperature. The Seebeck coefficients of PEI-SWNT (N) at all temperatures were represented as negative values, indicating that the major charge carriers in SWNTs are electrons by hole blocking in the valence band and electron injection into the conduction band under n-type doping mechanism.[33]

Furthermore, power factor ($S^2\sigma$) was calculated by multiplying the square of Seebeck coefficient with the electrical conductivity. This is a significant factor that represents the performance of a thermoelectric material. In case of acid-treated SWNT (P1) and PEI-SWNT (N), the temperature dependence of power factor similarly followed the tendency of their electrical conductivities. On the other hand, the power factor of urea-SWNT (P2) relied on the tendency of its Seebeck coefficients.

We piled the buckypapers of p-type sample (urea-treated SWNT) and n-type sample (PEI-SWNT) alternatively, so as to construct p-n junctions, *i.e.* a thermoelectric module for power generation (Figure 3(a)). The Seebeck coefficient and resistance of the piled p-n couples were analyzed upto four layers, as shown in Figure 3(b) and (c). At each measurement temperature, the resistance and Seebeck coefficinet were increased as the number of layers was increased. The resistance of the p-n couples was found to be smaller at higher temperature, with the Seebeck coefficient being almost constant in the whole temperature ranges. The generated thermoelectric voltages were also measured as a function of temperature gradient, as shown in Figure 3(d). Generally, the voltages were increased linearly with ΔT. With increase in the number of p-n couples stacked in series, the generated voltage was found to increase up to 7.5 mV at a temperature gradient of 50 K. The highest ther-

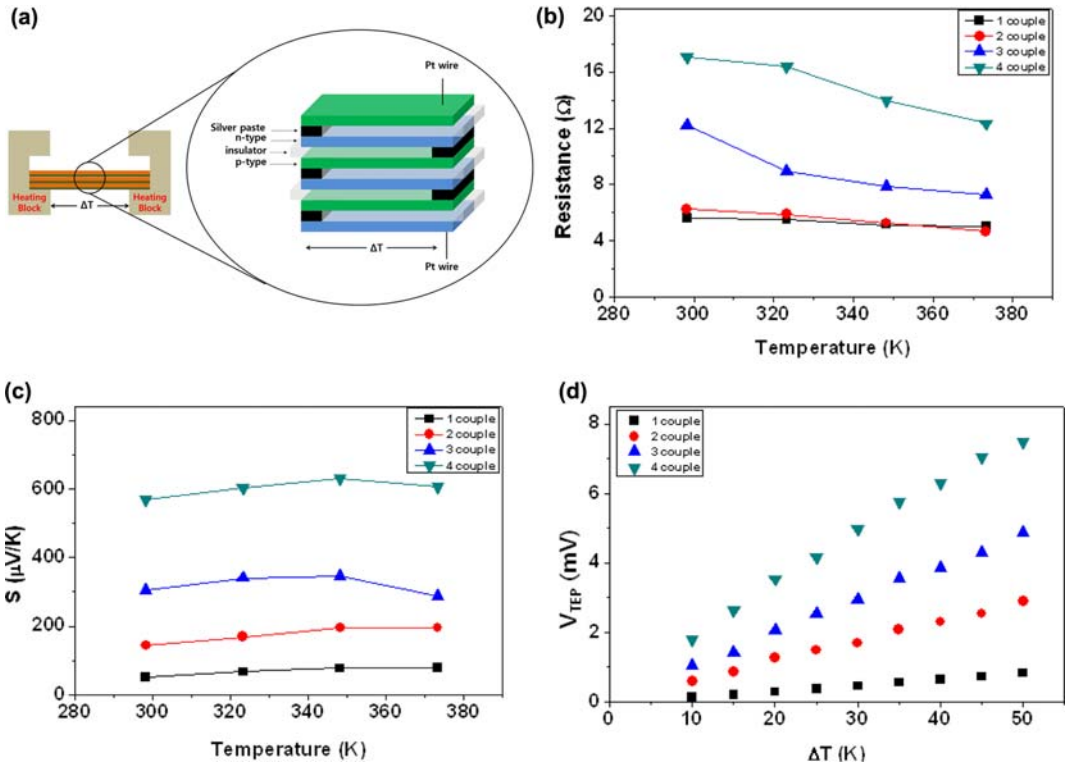

Figure 3. (a) Schematic diagram of the module fabricated with p/n couples. (b) Resistance, (c) Seebeck coefficient and (d) resistance of a thermoelectric module fabricated with one to four layers of p-type SWNTs (urea-SWNT, P2) and n-type SWNTs (PEI-SWNT, N).

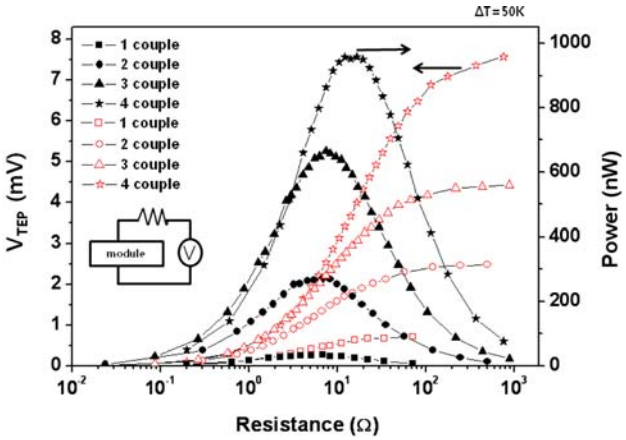

Figure 4. Generated thermoelectric voltage and thermopower for one to four p-n junctions connected in series, obtained at a temperature gradient of 50 K for varying load resistance.

moelectric voltages of 1, 2, 3, and 4 couples were 0.83, 2.9, 4.9 and 7.5 mV at ΔT=50 K, respectively.

Besides, for every p-n couple, we measured the generated thermoelectric voltage (V_{TEP}) of each p-n couple at a temperature gradient of 50 K, for various load resistance. Subsequently, thermal power (P) was calculated by V^2/R. As evidenced from Figure 4, each p-n couple generated a voltage of 0.7 mV and the corresponding generated power was 35 nW. With the stacking of p-n couples, the generated voltage increased up to 7 mV and the corresponding generated power was 960 nW. The maximum power outputs of 1, 2, 3, and 4 p-n couples were about 33 (at 5 Ω), 270 (at 6 Ω), 660 (at 8 Ω), and 960 nW (at 17 Ω), respectively. These data indicates that the maximum power output can be generated with a specific loaded resistance in a circuit. Comparing with recent literature reports related with SWNTs, this power output is about 40 times higher than that (~25 nW) of three p-n couples made by SWNTs[21] or about seven times higher than that (~137 nW) of 72 layer film of MWNTs.[23] Even though the voltages generated by temperature gradient were slightly lower than that of reported data, we obtained very high power output due to considerably low internal resistance. We believe that the power output of the thermoelectric module can be increased even further by increasing the number of p-n couples in the thermoelectric module.

Conclusions

In conclusion, p-type and n-type SWNTs were prepared by dip coating acid-treated SWNTs in urea and PEI, respectively. The electrical conductivity of urea-SWNT was found to be almost 3 times greater than that of acid-treated SWNT, whereas the Seebeck coefficient of urea-SWNT was lower than that of acid-treated SWNT at 298 K. The electrical conductivity of acid-treated SWNT was found to decrease with increase in temperature. This phenomenon could be mainly attributed to the backscattering of charged carriers and the high thermal expansion coefficient of SWNT buckypapers. However, the electrical conductivity of PEI-SWNT was found to increase in the temperature of 298 to 373 K. A small thermoelectric module was obtained by alternatively stacking the p-n couples and their thermoelectric voltages and power output were also investigated. The thermoelectric voltages were increased as ΔT was larger and the maximum power output was reached to approximately 1000 nW with four p-n couples, applying ΔT=50 K.

Acknowledgments. H. Lee acknowledges the financial support for this work given by the National Research Foundation of Korea Grant funded by the Korean Government (MEST) (2014R1A1A3052933 and 2015R1A5A7037615).

Supporting Information: Schematic diagram for preparation of carbon nanotubes thin film p/n junctions doped with N-containing organic molecules; Schematic diagram (a) for electrical conductivity measurement (4-Point-Probe method), Carrier concentration and carrier mobility of p-type SWNTs (acid-treated SWNT and urea-SWNT, P1 and P2) and n-type SWNTs (PEI-SWNT, N). (b) Seebeck coefficient measurement; The materials are available *via* the Internet at http://www.springer.com/13233.

References

(1) F. J. DiSalvo, *Science*, **285**, 703 (1999).
(2) B. Poudel, Q. Hao, Y. Ma, Y. C. Lan, A. Minnich, B. Yu, X. A. Yan, D. Z. Wang, A. Muto, D. Vashaee, X. Y. Chen, J. M. Liu, M. S. Dresselhaus, G. Chen, and Z. F. Ren, *Science*, **320**, 634 (2008).
(3) D.-Y. Chung, T. Hogan, P. Brazis, M. Rocci-Lane, C. Kannewurf, M. Bastea, C. Uher, and M. G. Kanatzidis, *Science*, **287**, 1024 (2000).
(4) Y. Zhai, T. Zhang, Y. Xiao, J. Jiang, S. Yang, and G. Xu, *J. Alloys Compd.*, **563**, 285 (2013).
(5) K. Biswas, J. He, Q. Zhang, G. Wang, C. Uher, V. P. Dravid, and M. G. Kanatzidis, *Nat. Chem.*, **3**, 160 (2011).
(6) Q. Zhang, C. D. Malliakas, and M. G. Kanatzidis, *Inorg. Chem.*, **48**, 10910 (2009).
(7) O. Bubnova, Z. U. Khan, A. Malti, S. Braun, M. Fahlman, M. Berggren, and X. Crispin, *Nat. Mater.*, **10**, 429 (2011).
(8) K.-C. Chang, M.-S. Jeng, C.-C. Yang, Y.-W. Chou, S.-K. Wu, M. Thomas, and Y.-C. Peng, *J. Electron. Mater.*, **38**, 1182 (2009).
(9) O. Bubnova, M. Berggren, and X. Crispin, *J. Am. Chem. Soc.*, **134**, 16456 (2012).
(10) S. Iijima, *Nature*, **354**, 56 (1991).
(11) T. Park, C. Park, B. Kim, H. Shin, and E. Kim, *Energy Environ. Sci.*, **6**, 788 (2013).
(12) W. Zhao, S. Fan, N. Xiao, D. Liu, Y. Y. Tay, C. Yu, D. Sim, H. H. Hng, Q. Zhang, F. Boey, J. Ma, X. Zhao, H. Zhang, and Q. Yan, *Energy Environ. Sci.*, **5**, 5364 (2012).
(13) J. Wu, Y. Sun, W. Xu, and Q. Zhang, *Synth. Met.*, **189**, 177

(2014).
(14) W. Lee, Y. J. Cho, H. R. Choi, H. J. Park, T. Chang, M. Park, and H. Lee, *J. Sep. Sci.*, **35**, 3250 (2012).
(15) M. Piao, J. Na, J. Choi, J. Kim, G. P. Kennedy, G. Kim, S. Roth, and U. Dettlaff-Weglikowska, *Carbon*, **62**, 430 (2013).
(16) J. Choi, N.K. Tu, S.-S. Lee, H. Lee, J. Kim, and H. Kim, *Macromol. Res.*, **22**, 1104 (2014).
(17) T. W. Ebbesen, H. J. Lezec, H. Hiura, J. W. Bennett, H. F. Ghaemi, and T. Thio, *Nature*, **382**, 54 (1996).
(18) S. Xie, W. Li, Z. Pan, B. Chang, and L. Sun, *J. Phys. Chem. Solids*, **61**, 1153 (2000).
(19) D. Kim, Y. Kim, K. Choi, J. C. Grunlan, and C. Yu, *ACS Nano*, **4**, 513 (2009).
(20) C. Yu, K. Choi, L. Yin, and J. C. Grunlan, *ACS Nano*, **5**, 7885 (2011).
(21) C. Yu, A. Murali, K. Choi, and Y. Ryu, *Energy Environ. Sci.*, **5**, 9481 (2012).
(22) H. S. Lee, C. H. Yun, S. K. Kim, J. H. Choi, C. J. Lee, H.-J. Jin, H. Lee, S. J. Park, and M. Park, *Appl. Phys. Lett.*, **95**, 134104 (2009).
(23) C. A. Hewitt, A. B. Kaiser, S. Roth, M. Craps, R. Czerw, and D. L. Carroll, *Nano Lett.*, **12**, 1307 (2012).
(24) J. Zhao, H. Park, J. Han, and J. P. Lu, *J. Phys. Chem. B*, **108**, 4227 (2004).
(25) C. Wang, G. Zhou, H. Liu, J. Wu, Y. Qiu, B.-L. Gu, and W. Duan, *J. Phys. Chem. B*, **110**, 10266 (2006).
(26) T. Park, K. Sim, J. Lee, and W. Yi, *J. Nanosci. Nanotechnol.*, **12**, 5812 (2012).
(27) B. H. Kim, T. H. Park, S. J. Baek, D. S. Lee, S. J. Park, J. S. Kim, and Y. W. Park, *J. Appl. Phys.*, **103**, 096103 (2008).
(28) Y. X. Zhou, A. Gaur, S. H. Hur, C. Kocabas, M. A. Meitl, M. Shim, and J. A. Rogers, *Nano Lett.*, **4**, 2031 (2004).
(29) Z. Lei, L. Lu, and X. S. Zhao, *Energy Environ. Sci.*, **5**, 6391 (2012).
(30) O. Boffoue, A. Jacquot, A. Dauscher, B. Lenoir, and M. Stolzer, *Rev. Sci. Instrum.*, **76**, 053907 (2005).
(31) S. Biamino and C. Badini, *J. Eur. Ceram. Soc.*, **24**, 3021 (2004).
(32) R. B. Koizhaiganova, D. H. Hwang, C. J. Lee, S. Roth, and U. Dettlaff-Weglikowska, *Phys. Status Solidi B*, **247**, 2793 (2010).
(33) Y. Nonoguchi, K. Ohashi, R. Kanazawa, K. Ashiba, K. Hata, T. Nakagawa, C. Adachi, T. Tanase, and T. Kawai, *Sci. Rep.*, **3**, 3344 (2013).
(34) V. Skákalová, A. B. Kaiser, Y. S. Woo, and S. Roth, *Phys. Rev. B*, **74**, 085403 (2006).
(35) N. R. Raravikar, P. Keblinski, A. M. Rao, M. S. Dresselhaus, L. S. Schadler, and P. M. Ajayan, *Phys. Rev. B*, **66**, 235424 (2002).
(36) Z. Li, V. Saini, E. Dervishi, V. P. Kunets, J. Zhang, Y. Xu, A. R. Biris, G. J. Salamo, and A. S. Biris, *Appl. Phys. Lett.*, **96**, 033110 (2010).